Received: 8 February 2020 | Accepted: 15 November 2020

DOI: 10.1002/vzj2.20093

Vadose Zone Journal

ORIGINAL RESEARCH ARTICLE

Cover systems with synthetic water-repellent soils

Shuang Zheng[1,2] | **Xin Xing**[2] | **Sérgio D. N. Lourenço**[2] | **Peter J. Cleall**[3]

[1] Civil Engineering Company, China Construction Fourth Engineering Division Corporation, Shenzhen, China

[2] Dep. of Civil Engineering, The Univ. of Hong Kong, Hong Kong, China

[3] School of Engineering, Cardiff Univ., Cardiff, UK

Correspondence
Sérgio D. N. Lourenço, Dep. of Civil Engineering, The Univ. of Hong Kong, Hong Kong, China.
Email: lourenco@hku.hk

Assigned to Associate Editor Joerg Bachman.

Funding information
Research Grants Council, University Grants Committee, Grant/Award Numbers: 17205915, T22-603/15-N

Abstract

A cover system is a crucial component of engineered landfills, to minimize water percolation into the underlying waste. Capillary barriers are an alternative cover system, which has been widely used in the arid and semiarid regions as no cohesive, low-permeability materials are used. However, the performance of capillary barriers in tropical climate has been unsatisfactory (breakthrough observed). In recent years, synthetic water-repellent granular materials have drawn increasing attention due to their distinctive hydraulic behavior (inhibited water infiltration and high water entry pressure), suggesting they may also be used to improve the performance of cover systems. In this study, flume tests were conducted with inclined model slopes under artificial rainfall. By monitoring the surface runoff, lateral diversion, and basal percolation and conducting water balance analysis, the performance of monolithic cover, conventional capillary barrier, and water-repellent cover systems were evaluated. The study revealed that (a) the barrier effect and diversion capacity were significantly strengthened by induced water repellency, providing a promising solution to extend the application of capillary barrier covers; and (b) cover systems can be formed using one raw material to decrease the construction cost, by using synthetic water-repellent soil as the underlying layer.

1 | INTRODUCTION

A landfill cover system, or capping system, is a crucial component of engineered municipal or hazardous waste landfills, which is designed to prevent access or exposure to waste, minimize water percolation into the underlying waste, and control landfill gas emissions (EPD, 2019; USEPA, 2011). A variety of landfill cover systems have been developed worldwide, including resistive cover systems and alternative cover systems. Resistive cover systems normally use materials with low saturated hydraulic conductivity (typically 10^{-9} m s^{-1} or less) such as compacted clay layers (Albright et al., 2006; Benson, Daniel, & Boutwell, 1999) or geosynthetic composite liners (Bouazza, 2002) to reduce infiltration and basal percolation by increasing the overland runoff. Although the resistive cover systems appear technically efficient, questions regarding their high construction cost and long-term performance have been reported (Rayhani, Yanful, & Fakher, 2007; Sadek, Ghanimeh, & El-Fadel, 2007). Evapotranspiration (ET) cover systems, including monolithic covers and capillary barrier covers, have been proposed and implemented as technically feasible alternative capping systems with easy construction and low cost (Bareither, Foley, & Benson, 2016; Barnswell & Dwyer, 2012). The ET covers serve not as a barrier, but as a reservoir that stores water during rainfall events

Abbreviations: DMDCS, dimethyldichlorosilane; ET, evapotranspiration; FDR, frequency domain reflectometry; SDM, sessile drop method; SWRC, soil water retention curve; WDPT, water drop penetration time; WEP, water entry pressure; WRC_1, Water-repellent Cover 1; WRC_2, Water-repellent Cover 2.

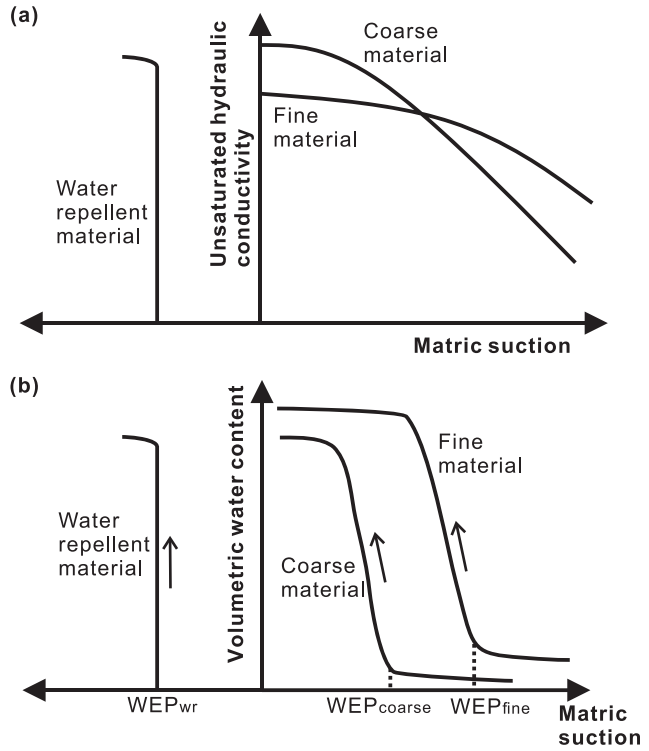

FIGURE 1 Conceptual illustration of the unsaturated hydraulic properties of sand, silt, and water-repellent sand: (a) unsaturated hydraulic conductivity function (after Dell'Avanzi et al., 2010), and (b) soil water retention curves (wetting branch; after Wang et al., 2000). Note: WEP is water entry pressure

and then releases it in the form of lateral drainage or evapotranspiration. A monolithic design is a single layer of geomaterial placed directly on the waste, where silts and clays of low plasticity are commonly used materials (Zornberg, LaFountain, & Caldwell, 2003). In contrast, a typical capillary barrier is composed of a layer of fine soil (usually silty or clayey soil) overlaying a layer of coarse soil (sandy or gravelly soil). The unsaturated hydraulic conductivity of the coarse-grained layer is smaller than that of the fine-grained layer, as presented in Figure 1a, and therefore a barrier against water flow is formed at the interface of the two layers, enhancing the water retention capacity of the upper fine soil layer (Khire, Benson, & Bosscher, 1999; Stormont & Anderson, 1999). Water then accumulates above the interface with the water content increasing and suction decreasing. Percolation into the lower layer (breakthrough) does not occur until the pressure at the interface reaches the water entry pressure (WEP) of the coarse-grained layer (WEP_{coarse}, Figure 1b). Capillary barrier covers have been investigated and are considered to work in arid and semiarid regions; however, the performance in tropical climates has been unsatisfactory, where intense and frequent precipitation is expected (Khire, Benson, & Bosscher, 2000).

To extend the application of capillary barrier covers to tropical and subtropical regions, several enhanced cover systems have been proposed (Table 1). Ng, Liu, Chen, and Xu (2015) proposed a three-layer capillary barrier cover system, where a soil layer with low permeability (a compacted clay layer) was added below a conventional capillary barrier (silt layer and gravelly sand layer). The compacted clay layer was able to prevent further penetration of water after breakthrough of the upper two layers, and water was laterally diverted within the gravelly sand layer due to the presence of the compacted clay layer. A similar approach was shared by Stormont and Morris (1997) to promote the lateral diversion capacity of a capillary barrier. An unsaturated drainage layer (fine-grained sand) was added at the finer–coarser interface of a capillary barrier, with the lateral diversion of accumulated water above the capillary barrier significantly improved. Harnas, Rahardjo, Leong, and Wang (2014) also proposed a dual capillary barrier system, which was reported to have stored more water before breakthrough as compared with the single capillary barrier of same thickness. Due to the increased water retention capacity, the dual capillary barrier is expected to outperform the normal capillary barrier. Nevertheless, additional soil layers are required to construct these capillary barrier cover systems, which may lead to increasing costs for construction and maintenance. An alternative landfill cover system that promotes a capillary barrier effect without inserting additional soil layers is desired.

Synthetic water-repellent soils, which show low affinity for water, have been reported to delay or restrict infiltration (Doerr et al., 2006), with increased WEP (Wang, Wu, & Wu, 2000), altered unsaturated hydraulic conductivity function (Dell'Avanzi, Guizelini, da Silva, & Nocko, 2010), and affected soil water retention curve (Wijewardana et al., 2016). The wetting path of soil water retention curve is strongly affected by the water repellency. With the increase of soil water repellency, the corresponding matric suction to the same water content decreases, whereas similar behaviors of both wettable and water-repellent soils were observed during drying processes, implying minimal effects of water repellency on the drying path of soil water retention curve (Czachor, Doerr, & Lichner, 2010). Due to the distinctive hydraulic properties (Figure 1) and infiltration characteristics, synthetic water-repellent soils may be used in a variety of applications in ground engineering (e.g., pavement base for roads, water harvesting facilities, and slope stabilization;

Core Ideas

- Barrier effect and diversion capacity are strengthened by water repellency.
- Release of water into underlying layer was inhibited even after breakthrough.
- A barrier can be formed with one raw material by using water-repellent soil.

TABLE 1 Summary of enhanced capillary barrier cover systems

Enhanced capillary barrier cover systems	Configuration (from top to bottom)	Reference
Three-layer capillary barrier	Silt layer + compacted clay layer + gravelly sand layer	Ng et al. (2015a)
Dual capillary barrier	Fine-grained layer + coarse-grained layer + fine-grained layer + coarse-grained layer	Harnas et al. (2014)
Water-repellent cover	Natural sand layer + water-repellent sand layer	Dell'Avanzi et al. (2010)
Capillary barrier with an unsaturated drainage layer	Fine soil layer + sand layer (unsaturated drainage layer) + coarse soil layer	Stormont and Morris (1997)

Zheng et al., 2017). Recent research shows that synthetic water-repellent soils may also be used in cover systems to improve performance. Due to the positive WEP of synthetic water-repellent soils, water does not infiltrate into the underlying layer until a positive water head above the interface is developed, and therefore the performance of cover system is expected to be enhanced. Dell'Avanzi et al. (2010) presented the use of synthetic water-repellent sand and evaluated its performance as a cover system (Table 1). By carrying out two scaled model tests on a conventional capillary barrier and a water-repellent cover (replacing the underlying layer with water-repellent sand), the tests revealed that the overall performance of water-repellent cover was substantially better than the conventional one. Breakthrough occurred after 44 min of continuous rainfall for the conventional capillary barrier, whereas the water-repellent cover withstood rainfall of more than 2 h, highlighting its potential to be used in tropical regions with high precipitation. The infiltration characteristics of water-repellent cover have been investigated by carrying out a one-dimensional column test (Rahardjo et al., 2017), confirming that the contrast in hydraulic conductivity of two layers gave rise to the barrier effect. However, the work of Dell'Avanzi et al. (2010) and Rahardjo et al. (2017) were preliminary with no overall evaluation of the performance of the water-repellent cover system, and a more detailed investigation is still necessary.

This study aims to evaluate the performance of a water-repellent cover system, by conducting model tests in an inclined flume under artificial rainfall. The specific objective of this study is to quantitatively analyze and compare the behavior of a monolithic cover, conventional capillary barrier and water-repellent covers, including surface runoff, lateral diversion, and basal percolation. The results will inform whether a satisfactory cover system can be constructed by using water-repellent materials.

2 | MATERIALS AND METHODS

2.1 | Soil description

Two industrial granular materials with different grain sizes are adopted in this study: Fujian sand (China ISO standard sand) and crushed silica (silt), as similar materials were used in previous study (Ng, Liu, Chen, & Xu, 2015). Fujian sand is a clean, siliceous sand consisting preferably of rounded particles with a silica content ≥98%. Its particle size distribution complies with ISO 679:2009 and is classified as poorly graded sand, as displayed in Figure 2. Crushed silica has the same composition as Fujian sand and is crushed with a median size of 20 μm. The grain size distribution of crushed silica is obtained using a particle size and shape analyzer (QICPIC, Sympatec) and presented in Figure 2 as well. The physical properties of Fujian sand and crushed silica are summarized in Table 2.

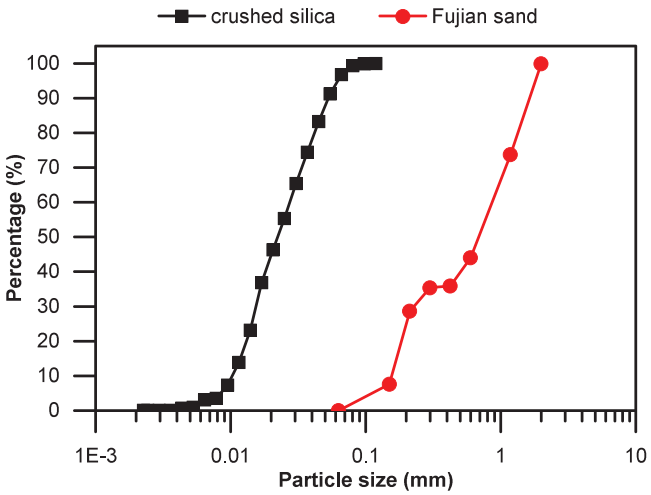

FIGURE 2 Particle size distributions of Fujian sand and crushed silica

TABLE 2 Physical properties of Fujian sand and crushed silica

Properties	Fujian sand	Crushed silica
Specific gravity, G_s	2.66	2.68
Max. void ratio, e_{max}	0.56	1.74
Min. void ratio, e_{min}	0.42	0.68
Coefficient of uniformity, Cu	5.56	2.80
Coefficient of curvature, Cc	0.34	0.86
Organic matter content, %	0.16	0.52
Natural contact angle, α	20.3 ± 2.6°	71.1 ± 5.3°

2.2 | Soil water repellency measurement

The level of water repellency of soil samples was assessed using two methods in this study: sessile drop method (SDM) and water drop penetration time (WDPT). The SDM is used to measure the contact angle of water drop on a soil sample surface. Contact angle is a direct expression of the wettability of surfaces: the intrinsic contact angle of a wettable surface is smaller than 90°, whereas a water-repellent (hydrophobic) surface has intrinsic contact angle greater than 90° (Bachmann, Woche, Goebel, Kirkham, & Horton, 2003). The procedures were introduced by Bachmann, Ellies, and Hartge (2000) and improved by Saulick, Lourenço, and Baudet (2017) as follows: sprinkling the soil on a double-sided adhesive tape fixed on a glass slide, removing the excess particles to ensure a monolayer of particles is fixed and any motion of the particles is prevented, placing the slide on a goniometer's stage, and dispensing a droplet of deionized water (10 μl) on the sample. Contact angle measurements are then performed with a goniometer (DSA 25, KRÜSS), by analyzing the shape of the droplet.

The WDPT is an index test that evaluates the persistency of soil water repellency. The test involves dispensing a drop of deionized water (50 μl) on the surface of prepared soil sample and recording the time for the water drop to completely infiltrate (Doerr, 1998). For wettable soils the water drop should penetrate immediately, and for water-repellent soils, the stronger the water repellency, the longer the time it takes to fully infiltrate. Based on the penetration time, the water repellency of soils can be classified into different categories, from wettable to extremely water repellent.

2.3 | Soil treatment

Soil water repellency is normally induced by coating the surface of soil particles with low-surface-energy substances in the laboratory, with a wide range of treatment agents introduced in the literature (Chan & Lourenço, 2016). Silane compounds are among the most suitable agents to achieve persistent and stable water repellency (e.g., dimethyldichlorosilane [Shaw, 1992], trimethylchlorosilane [Laskowski & Kitchener, 1969], and octadecyltrichlorosilane [McGovern, Kallury, & Thompson, 1994]). The silanes share a similar reaction mechanism, which is that the silanes react with water, to form water-repellent polymers bonding to the soil particle surface. Recently, dimethyldichlorosilane (DMDCS) has been frequently used to form water-repellent coatings on soil samples (Bachmann et al., 2000; Ng & Lourenço, 2016), due to the simplicity of sample preparation (no solvent needed) and persistent water repellency. Therefore, DMDCS is adopted in this study.

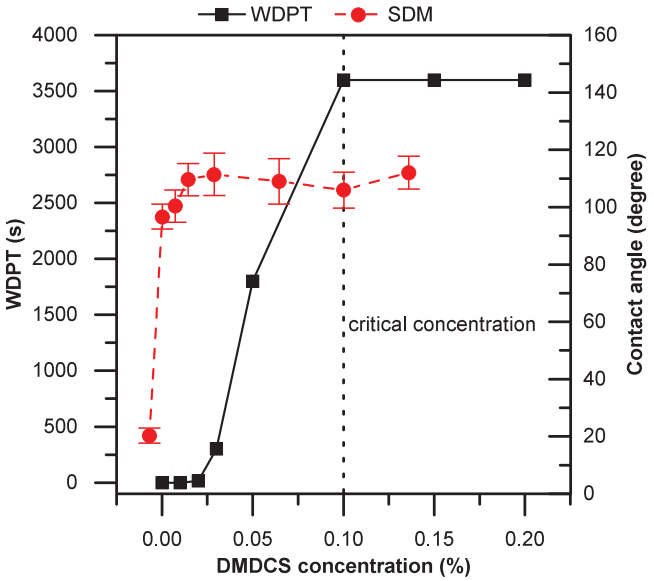

FIGURE 3 Change in water drop penetration time (WDPT) and contact angle with dimethyldichlorosilane (DMDCS) concentration for Fujian sand

In this study, synthetic water-repellent soils are prepared using dry soils, after adding DMDCS, the soil is thoroughly mixed to guarantee a uniform distribution of water repellency. Before carrying out a flume test, several samples were taken and the level of soil water repellency are assessed (i.e., contact angle and water drop penetration time, to further confirm the magnitude and persistency of water repellency, respectively). The concentration of DMDCS required to reach extreme water repellency is dependent on soil type. Ju, Ren, and Horton (2008) applied 16.8 ml kg^{-1} for the loam soil and 84 ml kg^{-1} for the silty loam soil to produce extremely water-repellent soils. Ng and Lourenço (2016) found that the maximum contact angle can be induced by 3% and 0.005% DMDCS by soil mass for alluvium and Leighton Buzzard sand, respectively. In this study, preliminary testing showed that the concentration of DMDCS to attain extreme water repellency in Fujian sand was 0.1% by soil mass (the cost of treating 1 metric ton of Fujian sand is approximately US$64), with a contact angle of 111° (Figure 3).

Experiments and estimations are conducted to obtain the hydraulic properties of soils involved in this study. The water entry pressure of water-repellent sand was measured by using water ponding method (Wang et al., 2000), with a positive WEP of 6.3 cm water head recorded. The Arya–Paris model (Antinoro, Bagarello, Ferro, Giordano, & Iovino, 2014) and van Genuchten model (Wang, François, & Lambert, 2020) are known for accurately estimating the soil water retention curves (SWRC) of silty soil and sandy soil, respectively, and therefore are adopted for obtaining the SWRC of crushed silica and Fujian sand, respectively. The SWRC curves of Fujian sand, crushed silica, and water-repellent Fujian sand

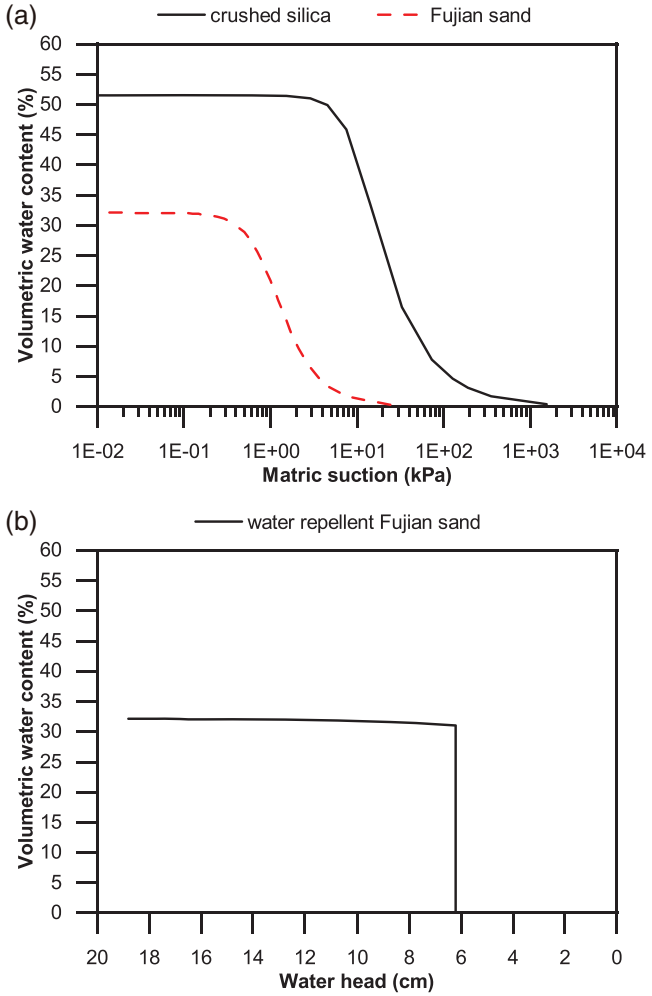

FIGURE 4 Soil water retention curves of (a) Fujian sand and silt (drying branch) and (b) water-repellent Fujian sand (wetting branch)

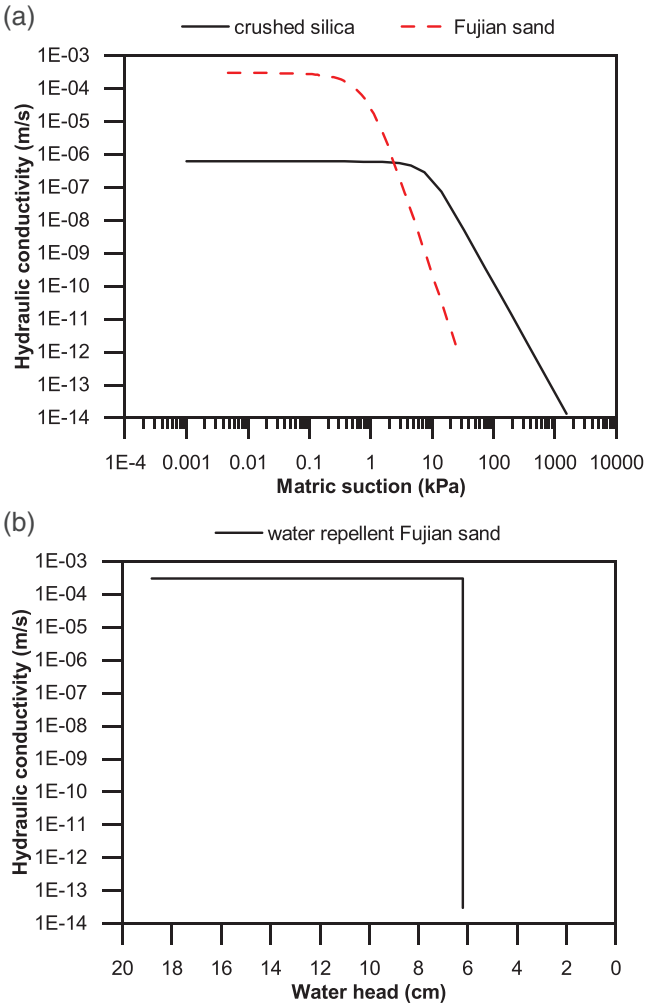

FIGURE 5 Unsaturated hydraulic conductivity function of (a) Fujian sand and silt and (b) water-repellent Fujian sand

are presented in Figure 4. Saturated hydraulic conductivity of crushed silica and Fujian sand were measured according to BS 1377-5:1990, as 6.16×10^{-4} m s^{-1} and 3.0×10^{-7} m s^{-1} respectively. Based on the saturated hydraulic conductivity and estimated SWRC, the unsaturated hydraulic conductivity functions of Fujian sand, crushed silica, and water-repellent Fujian sand are determined by using van Genuchten–Mualem model (Wang et al., 2019), as summarized in Figure 5.

2.4 | Flume test

2.4.1 | Flume configuration

The inclined flume model has been a well-established approach to investigate the performance of sloping covers with a capillary barrier effect (Damiano, Greco, Guida, Olivares, & Picarelli, 2017; Ng, Liu, Chen, & Xu, 2015). In this study, a Perspex-sided flume was manufactured with the dimensions of 80 cm long, 40 cm wide, and 25 cm deep, to simulate several cover systems. Artificial rainfall is generated using a rainfall simulator, which consisted of a nozzle (Full-Jet, Spraying Systems), a flowmeter and a control valve to ensure constant rainfall intensity during tests. A video camera (HERO4 Silver, GoPro) was positioned parallel to the side to capture the downward movement of wetting front. Ten frequency domain reflectometry (FDR) soil moisture sensors (EC-5, Decagon Devices) were deployed at various depths (3, 8, 13, 18, and 23 cm) to monitor the change in soil water content. To separate and collect the surface runoff, lateral diversion, and basal percolation during the experiment, four openings were cut and connected to plastic hoses at the downstream boundary of each soil layer. Figure 6 shows the configuration of the flume and instrumentation.

2.4.2 | Test preparation and procedures

The flume model consisted of three layers. The two upper layers formed the capillary barrier system (the material varied among tests) and a gravel layer underneath to facilitate

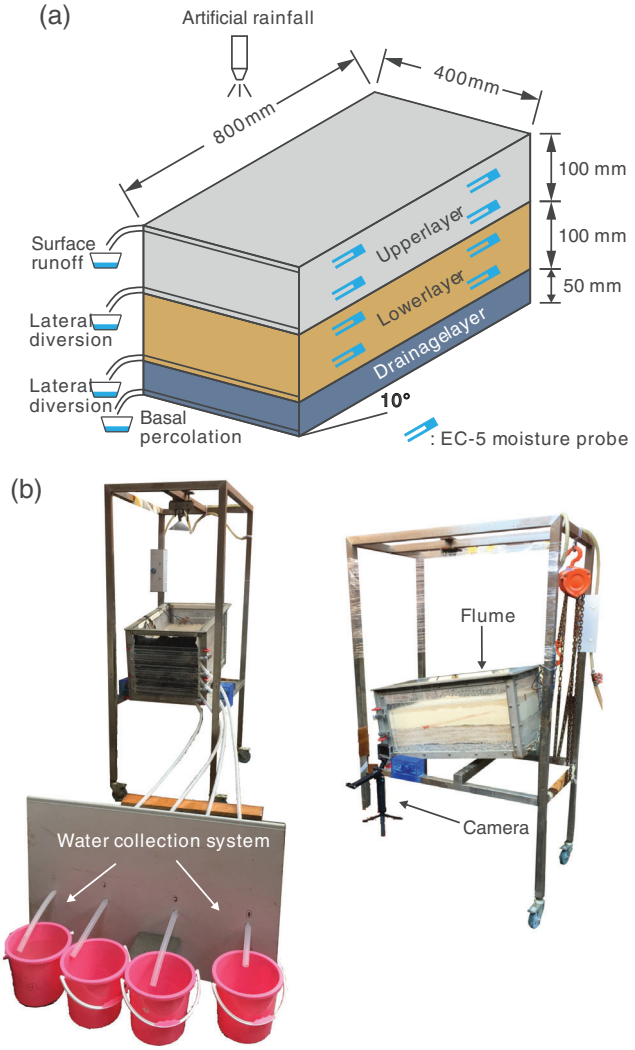

FIGURE 6 Configuration of flume: (a) schematic illustration of dimensions and instruments, and (b) view of the flume

drainage. The soils used to fill the model were deposited in a horizontal orientation (i.e., slope angle of zero) with a thickness of 1 cm at a time, to reduce the variation in density. For crushed silica, the dry density was controlled to be 1.30 g cm^{-3}. Five percent of water was added, and the crushed silica was thorough mixed before deposited in the flume, followed by compaction of controlled energy to achieve designated density. For Fujian sand, no water was added in order to observe the wetting front clearly, and a dry density of 1.80 g cm^{-3} was achieved. A sheet of nonwoven geotextile was placed at each interface of soil layers to prevent particles from migrating into the other layer. As indicated by Ng, Liu, Chen, and Xu (2015), its vertical saturated hydraulic conductivity was much higher than those of soils used, and therefore the influence on infiltration can be ignored. After the soils were filled, the flume was tilted to a slope angle of 10°.

The data logger, video camera, and stopwatch were synchronized before the experiments began and started recording once the rainfall simulator was activated. A preliminary study showed that the steady state was reached within 240 min under 40 mm h^{-1} rainfall; therefore, the artificial rainfall lasted for 240 min for each test. During the tests, the surface runoff, lateral diversion in the upper two layers, and the basal percolation were measured separately at 10-min intervals, and the water was stored in the cover system was calculated accordingly. The spatial evolution of water content was traced by the FDR moisture sensors. The times at which the wetting front reached each interface and the breakthrough occurred were recorded. After the rainfall event, the diversion and percolation continued due to the release of water storage in the soil and were measured until decreased to zero.

2.4.3 | Testing scenarios

Four flume tests were carried out to investigate the effectiveness of water-repellent cover systems in this study, as listed in Table 3. Each test simulated a cover system (i.e. ,monolithic cover, conventional capillary barrier, and two water-repellent cover systems):

I. The monolithic cover used compacted crushed silica for both layers, and therefore no capillary barrier effect and delay in infiltration was expected at the interface.
II. The conventional capillary barrier was composed of a crushed silica layer and an underlying Fujian sand layer, to simulate the capillary barrier cover constructed in arid areas.
III. The Water-repellent Cover 1 (WRC_1) was constructed by replacing the sand layer in the conventional capillary barrier with a water-repellent sand layer, to further enhance the effect of the capillary barrier (e.g., extended breakthrough time and increased water storage in the upper layer).
IV. The Water-repellent Cover 2 (WRC_2) consisted of a Fujian sand layer and an underlying water-repellent Fujian sand layer, where the barrier effect was not due to different particle sizes but contrasting hydraulic properties (wettable vs. water repellent).

3 | RESULTS

To describe and compare the hydrological responses of the cover systems, the time series data of all four tests were analyzed and presented in Figures 7–9, including the downward movement of wetting front (Figure 7), the change in volumetric water content at slope crest (Section I) and slope toe (Section II) (Figure 8), and the summary of temporal change in surface runoff rate, basal percolation rate, and lateral diversion rates in the upper layer and lower layer (Figure 9). The time when the wetting front reached the interface and base was

TABLE 3 Summary of settings and results of flume test

Test No.	Test settings		Test results							
	Upper layer	Lower layer	T_{in}	T_{br}	T_{ba}	V_r	V_{ld1}	V_{ld2}	V_p	V_s
			min			%				
I. Monolithic cover	Crushed silica	Crushed silica	60	N/A	129	28.3	0	0.8	4.4	66.6
II. Conventional capillary barrier	Crushed silica	Fujian sand	55	65	91	47.9	0.2	1.1	8.1	42.8
III. Water-repellent Cover 1	Crushed silica	Water-repellent Fujian sand	58	>240	>240	57.0	9.9	0	0	33.2
IV. Water-repellent Cover 2	Fujian sand	Water-repellent Fujian sand	35	>240	>240	0	60.3	0	3.5	36.3

Note. T_{in} denotes the time when wetting front reached the interface between two upper layers (10 cm deep); T_{br} denotes the time when breakthrough of capillary barrier occurred; T_{ba} denotes the time when wetting front reached the base of cover system (20 cm deep); V_r denotes the percentage of cumulative surface runoff; V_{ld1} denotes the percentage of cumulative lateral diversion in upper layer; V_{ld2} denotes the percentage of cumulative lateral diversion in lower layer; V_p denotes the percentage of cumulative basal percolation; V_s denotes the percentage of cumulative water storage; N/A, not applicable.

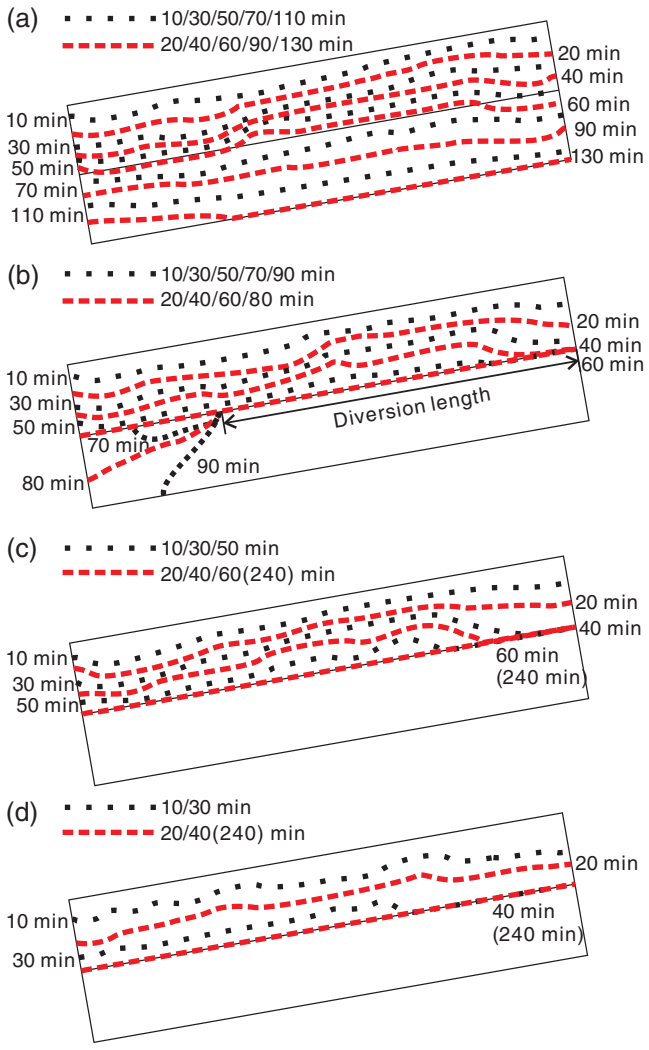

FIGURE 7 Wetting front movement with time: (a) monolithic cover, (b) conventional capillary barrier, (c) Water-repellent Cover 1, and (d) Water-repellent Cover 2

summarized in Table 3. The water balance analysis (including cumulative rainfall, cumulative surface runoff, cumulative lateral diversion, cumulative basal percolation and water storage) was conducted and exhibited in Figure 10.

3.1 | Wetting front movement

The downward movement of wetting front of all four tests are presented in Figure 7. For monolithic cover, a wetting front that was parallel to the slope surface and moved downwards was observed, it reached the interface at 60 min and the base at 130 min (Figure 7a). Figure 7b showed that the wetting front of conventional capillary barrier was parallel to the slope surface before reaching the silt–sand interface at 55 min. The infiltration was then prevented from entering the underlying sand layer because of the capillary barrier effect, with water accumulated above the interface. Figures 7c and 7d showed that the wetting front movement pattern of WRC_1 and WRC_2 were similar. The wetting front of WRC_1 and WRC_2 were parallel in the upper layer and reached the interface at 58 and 35 min, respectively. Due to the positive water entry pressure of the underlying water-repellent sand layer, the capillary barrier effect was significantly enhanced. Throughout the whole test, breakthrough did not occur and the wetting font remained at the interface.

3.2 | Volumetric water content

Figure 8 presented the change in volumetric water content at slope crest (Section I; Figures 8a, 8c, 8e, and 8g) and slope toe (Section II; Figures 8b, 8d, 8f, and 8h) of four tests. The straight lines of water content across the interface between 80- and 130-mm depth were not realistic, as water content was only measured at designated depths. The results of monolithic cover (Figures 8a and 8b) agreed with the observation of wetting front (Figure 7a): shallower sensors tracked a rise of readings at first (from 1 to 42%), followed by deeper sensors. The time when sensor reading suddenly increased was correlated with the depth, suggesting that wetting front was moving at a nearly constant velocity. Slope inclination of 10° had little influence on infiltration, as the change in volumetric water content with depth at slope toe (Figure 8b), followed a similar trend as at slope crest (Figure 8a).

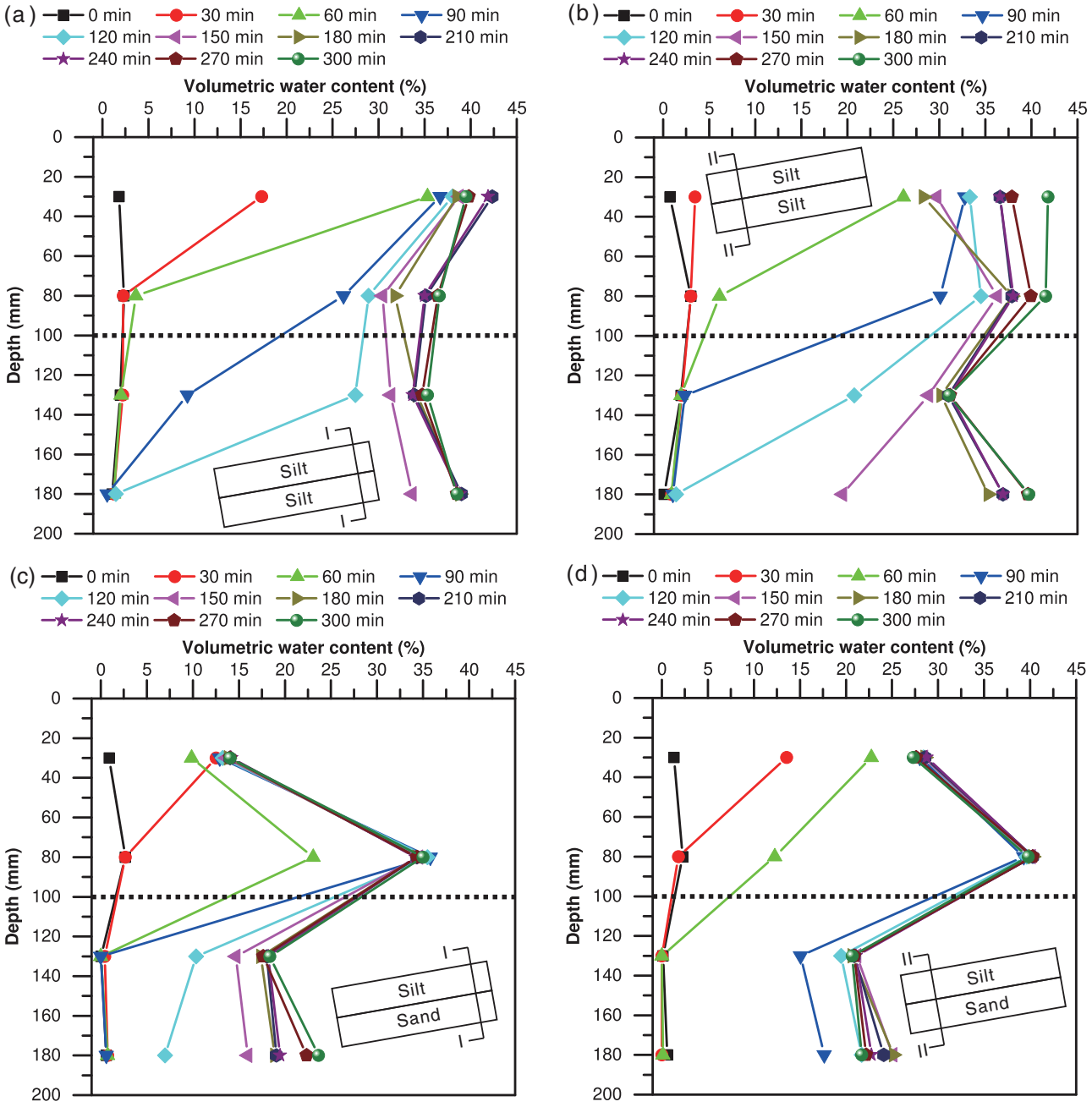

FIGURE 8 Change in volumetric water content: (a) slope crest (Section I) of monolithic cover; (b) slope toe (Section II) of monolithic cover; (c) slope crest (Section I) of conventional capillary barrier; (d) slope toe (Section II) of conventional capillary barrier; (e) slope crest (Section I) of Water-repellent Cover 1; (f) slope toe (Section II) of Water-repellent Cover 1; (g) slope crest (Section I) of Water-repellent Cover 2; and (h) slope toe (Section II) of Water-repellent Cover 2. Note: WR stands for water-repellent

The presence of capillary barrier effect was demonstrated by the results of conventional capillary barrier cover (Figure 8c and 8d). In the overlying silt layer, the water content at 80-mm depth was higher than that at 30-mm depth, owing to accumulated water above interface. The water content difference at slope crest and slope toe were 21 and 12%, respectively. The breakthrough of capillary barrier occurred at 65 min, and the wetting front moved further into the sand layer. It is worth noting that the breakthrough took place at a certain location (~57 cm) in the down-dip direction, which is often referred to as the diversion length or down dip limit (Ross, 1990), as plotted in Figure 7b. The accumulated water infiltrated into underlying layer, with the wetting zone expanding and the wetting front no longer parallel to surface. Although Figure 7b showed that breakthrough happened at the lower end of the model, leakage along the back side of

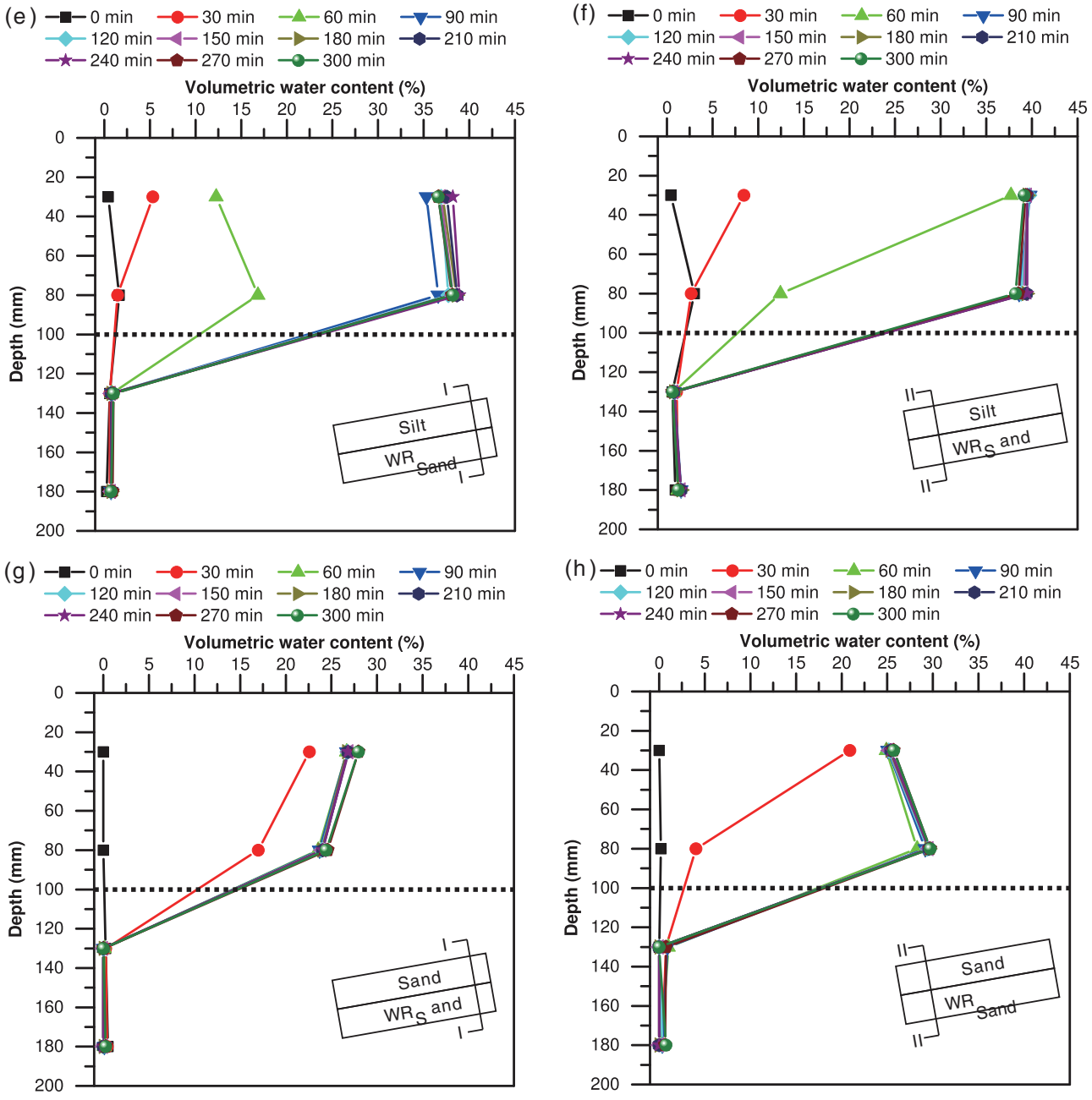

FIGURE 8 Continued

the flume was observed during the test, resulting in a rise in water content recorded by the moisture sensors buried in the sand layer of Section I (Figure 8c).

The results of WRC_1 and WRC_2 evidenced the improved capillary barrier effect of water-repellent soils. For WRC_1 and WRC_2, sensors in the upper layer recorded an increase as the wetting front moved downward, reaching a maximum water content of 37–40% (Figures 8e and 8f) and 24–30% (Figure 8g and 8h), respectively. However, the readings of sensors in the water-repellent sand layer remained unchanged till the end of rainfall event (240 min), as no infiltration into this layer took place.

3.3 | Water balance analysis

In Figure 9, temporal change in surface runoff rate, basal percolation rate, and lateral diversion rates in the upper layer and lower layer were summarized. The water balance analysis (including cumulative rainfall, cumulative surface runoff, cumulative lateral diversion, cumulative basal percolation, and water storage) was conducted and exhibited in Figure 10. For monolithic cover (Figure 9a), all rainfall infiltrated and no surface runoff was recorded at the beginning of the rainfall event, indicating that the initial infiltration capacity was greater than the rainfall intensity. Surface runoff was observed

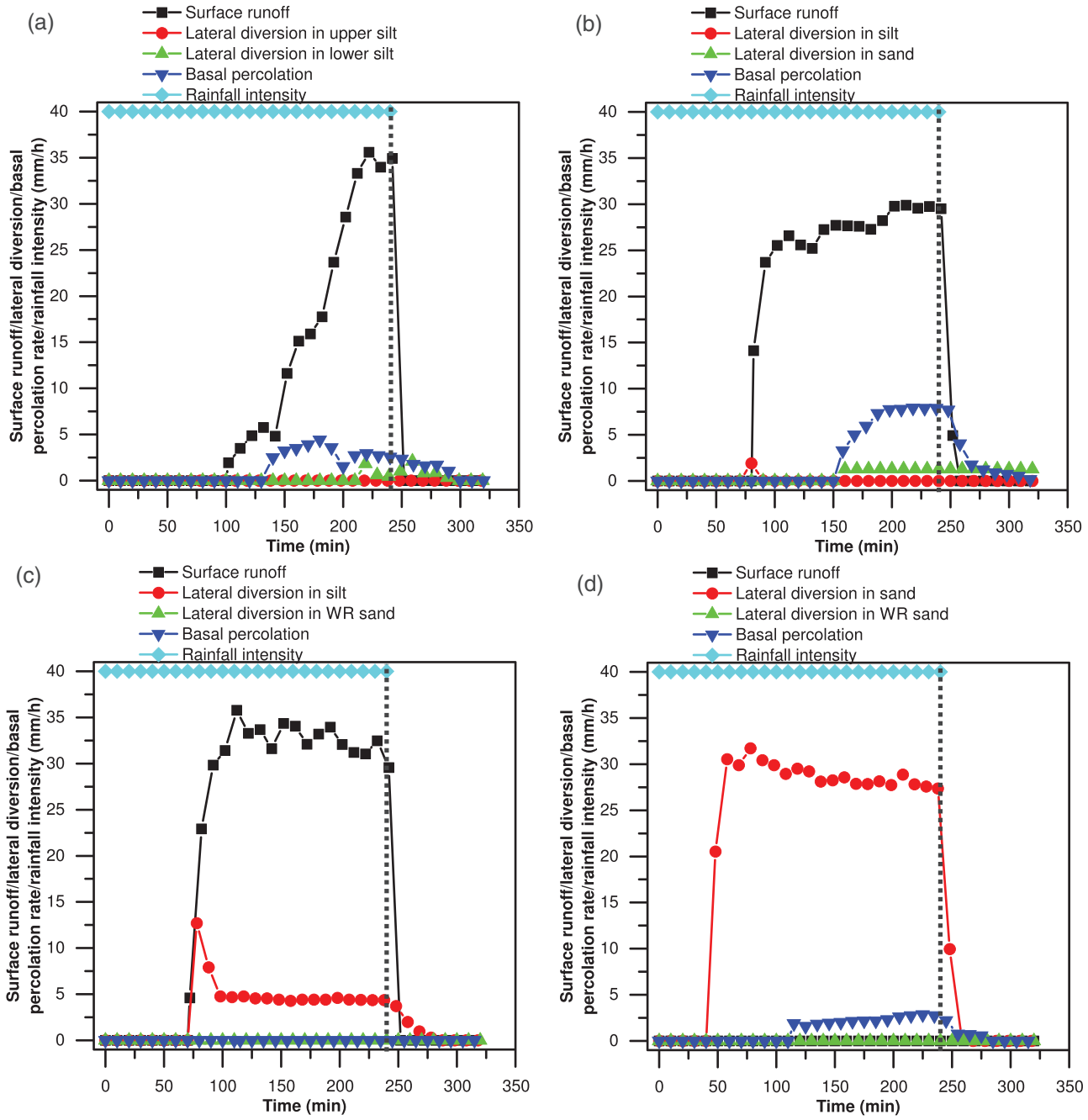

FIGURE 9 Temporal flow rates: (a) monolithic cover, (b) conventional capillary barrier, (c) Water-repellent Cover 1, and (d) Water-repellent Cover 2

at 92 min and experienced a sharp increase until reaching steady state of 35.6 mm h^{-1} at 222 min, corresponding to the steady state of water storage (114.6 mm) in the cover system (Figure 10a). The measured lateral diversion rate in upper silt layer was 0 mm h^{-1} throughout the test, whereas the lateral diversion in lower silt layer was recorded at 130 min, same as the time when wetting front reached the bottom. The lateral diversion was relatively little, with the maximum rate of 4.4 mm h^{-1}. After the rainfall stopped at 240 min (dashed line in Figure 9a), the surface runoff ceased immediately, whereas the lateral diversion in the lower silt layer and basal percolation gradually decreased to 0 mm h^{-1} within 300 min, which was attributed to released water storage (8.1 mm).

For conventional capillary barrier (Figure 9b), the infiltration rate was equal to the rainfall intensity at the beginning of test, and due to the capillary barrier effect, the appearance of surface runoff was accelerated to 72 min, followed by a drastic increase to 23.7 mm h^{-1} at 92 min, and a gentle increase to the steady state of 29.8 mm h^{-1} at 202 min. The lateral diversion in silt layer was only collected during 70–80 min, coinciding

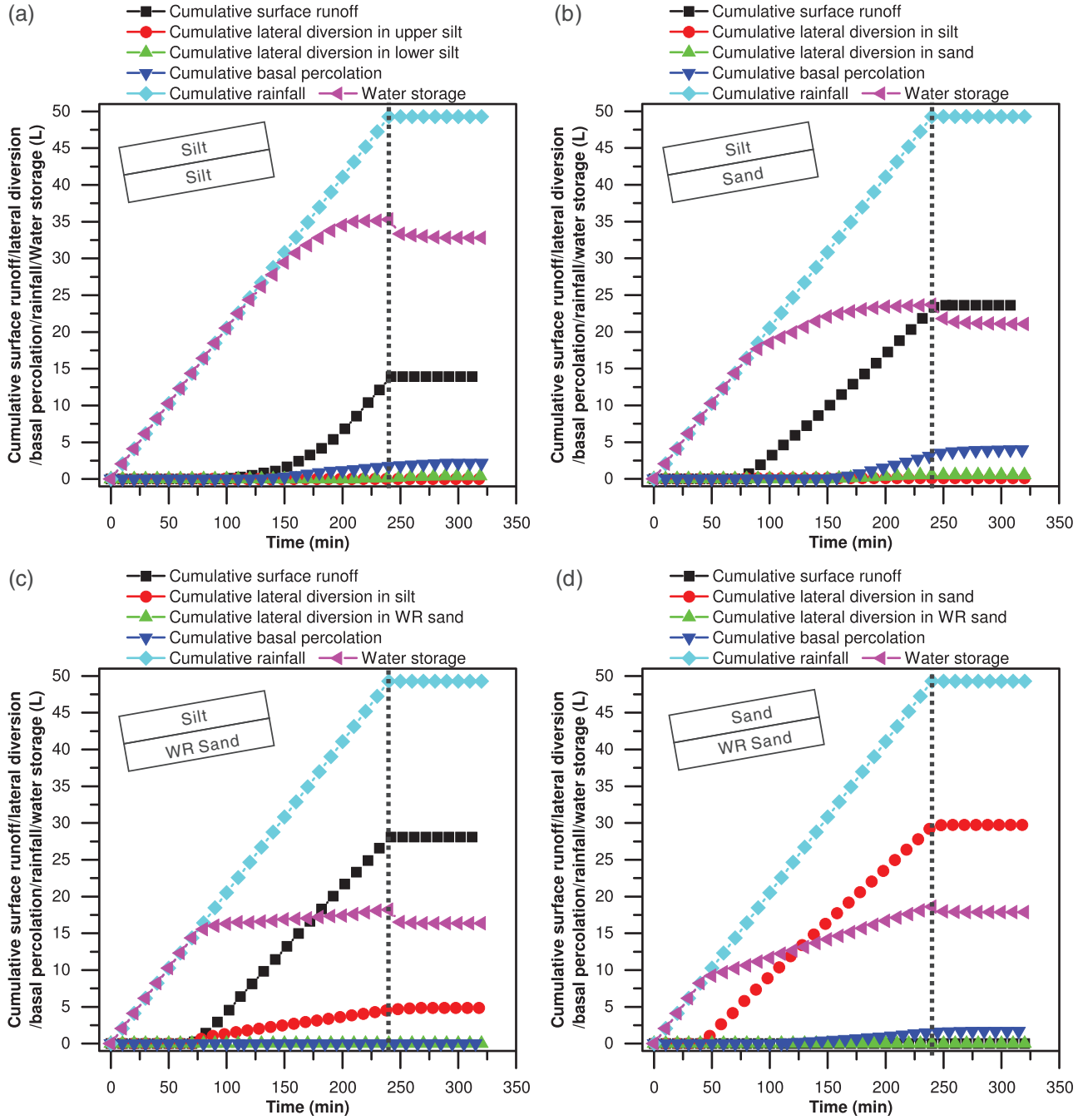

FIGURE 10 Water balance analysis of four cover systems: (a) monolithic cover, (b) conventional capillary barrier, (c) Water-repellent Cover 1, and (d) Water-repellent Cover 2. Note: WR stands for water-repellent

with the appearance of surface runoff, which indicated that the sloping capillary barrier effectively promoted the surface runoff and lateral diversion along the interface. After breakthrough, the lateral diversion in sand layer and basal percolation were observed nearly simultaneously (150 and 148 min), and reached a steady state of 1.3 and 7.9 mm h^{-1}. The water storage was 76.9 mm at the end rainfall event, smaller than that of the monolithic cover system (Figure 10b). The surface runoff ceased immediately after the rainfall ended, whereas 8.5 mm of stored water was released in the form of lateral diversion in the silt layer and sand layer.

Figure 9c showed that for WRC_1, as the simulated rainfall began, all rainwater infiltrated into the silt layer until surface runoff was collected at 62 min. The surface runoff rate achieved the maximum of 35.8 mm h^{-1} at 112 min, and then slightly decreased to 32.5 mm h^{-1} at 232 min. During the test, the infiltrated rainwater accumulated above the interface and was diverted along the inclined interface, leading to the

measured lateral diversion in silt layer after 68 min. No lateral diversion in the water-repellent sand layer and basal percolation was collected during the whole test; this result corroborated the fact that no breakthrough occurred. After the rainfall event, the water storage decreased gradually from 59.1 to 53.1 mm (Figure 10c), through lateral diversion in silt layer.

No surface runoff was collected during the test of WRC_2 (Figure 9d), suggesting that the infiltration capacity of Fujian sand was constantly greater than rainfall intensity (40 mm h^{-1}), where all rainwater infiltrated and was converted into lateral diversion. After the wetting front reached the interface at 35 min, the lateral diversion was collected at 38 min and quickly increased to 30.5 mm h^{-1} at 58 min, indicating that the water-repellent barrier effectively promoted the lateral diversion above the interface. The lateral diversion in water-repellent sand was 0 mm h^{-1} during the test. Nevertheless, basal percolation was measured at 105 min and gradually increased to 2.86 mm h^{-1} before the rainfall stopped. The unexpected percolation was investigated after the test by removing the material layer by layer, and several preferential flow paths (approximately 1–2 cm wide and corresponding to wet areas within the dry sand matrix) caused by transducer wires were identified in the water-repellent sand, which allowed the accumulated water to drain through the water-repellent sand layer. The preferential flow was not reflected by the wetting front or volumetric water content, as the flow paths were located in the center of soil mass and bypassed the soil moisture sensors (the measurement volume of EC-5 is 240 ml). After rainfall stopped, both lateral diversion in sand layer and basal percolation continued and gradually decreased to 0. At the end of this test, the cumulative basal percolation was 5.5 mm (Figure 10d), which was only 3.5% of the cumulative rainfall; most of the rainwater (96.5 mm, 60.3%) was diverted along the sand–water-repellent sand interface.

4 | DISCUSSION

4.1 | Conventional capillary barrier vs. Water-repellent Cover 1

The results clearly demonstrated that both conventional capillary barrier and WRC_1 can delay water infiltration and promote lateral diversion in cover systems, and the effectiveness of the WRC_1 system was noticeably greater. In a capillary barrier system, breakthrough is controlled by the WEP of the underlying coarse-grained material, and the promising performance of water-repellent cover stems from the positive WEP values. For conventional capillary barrier, with the water accumulated above the interface and the increase of water content, the matric suction decreases. Water then percolates into the underlying sand layer when the suction equals the estimated WEP of Fujian sand, ~7 kPa (Figure 4a). For WRC_1, the water content and suction in the silt layer experience similar processes, and the breakthrough would not occur until the water head equals the WEP of water-repellent sand (i.e., 6.3 cm water head; intersection between the curve and x axis in Figure 4b). The positive WEP (positive water head) of water-repellent sand implies much stronger ability to withstand percolation and divert rainwater. A positive water head has to build up above the interface to penetrate into the water-repellent sand layer. For a conventional capillary barrier cover, the barrier remains effective only if the matric suction is higher than a certain value (intersection of fine and coarse materials in Figure 1a).

The advantages of water-repellent covers are not limited to enhanced capillary barrier effect. In engineering practice, the long-term performance of conventional landfill covers was reported to deteriorate over time due to various issues—for example, the formation of cracks resulted from desiccation (Khire et al., 2000; Sadek et al., 2007), frost action (Albright et al., 2006), or differential settlement (Ling, Leshchinsky, Mohri, & Kawabata, 1998). Data collected from 10 field sites at the time of construction and 2–4 yr after construction indicated that the saturated hydraulic conductivity can increase by 10,000 times (Benson, Sawangsuriya, Trzebiatowski, & Albright, 2007), and Rayhani et al. (2007) reported a 12–34 times increase in hydraulic conductivity that was attributed to cracking. For water-repellent covers, as infiltration into the water-repellent layer is prevented, cracking induced by wet–dry and freeze–thaw cycling is avoided. On the other hand, the water-repellent layer is composed of dry, granular material, which can deform without impairing water repellency. Therefore, water-repellent covers are expected to accommodate uneven settlement of contained waste and minimize its damage to cover system. Even though the hydraulic conductivity of the upper fine-grained layer increases over time, the long-term performance of the water-repellent cover system is controlled by the water-repellent layer and is anticipated to outperform conventional landfill cover systems.

4.2 | Water-repellent Cover 1 vs. Water-repellent Cover 2

The intention of the WRC_2 test was to verify if a capillary barrier can be constructed using a single raw material to decrease the cost for construction and maintenance, with contrasting hydraulic properties provided by induced water repellency. The results proved that WRC_2 performed satisfactorily in promoting lateral diversion and minimizing basal percolation, even after the occurrence of breakthrough. Although the same material was adopted for the lower layer of both cover systems, no basal percolation was measured for WRC_1, whereas preferential flow was observed in WRC_2. A possible explanation was that the

preferential flow in WRC_2 was caused by high infiltration capacity of sand and increased water accumulation above interface (Figure 8g); subsequently, the WEP of water-repellent sand was reached and preferential flow paths formed. Ritsema and Dekker (2000) investigated water flow in the unsaturated zone of a water-repellent sandy soil, using numerical simulation with a two-dimensional flow and transport model. The study revealed that once the water pressure at the interface reached the WEP of the water-repellent soil, the front started to move downward, forming preferred pathways. Their study also indicated that preferential flow paths were only formed during infiltration into dry water-repellent soils, as in WRC_2. The results of WRC_2 demonstrated that for a water-repellent cover, infiltration into the underlying layer was still inhibited even after breakthrough happened, with much less basal percolation than a conventional capillary barrier system.

In addition, due to the coarse-grained surface layer with high infiltration capacity, less surface runoff is expected in WRC_2, which may result in decreased erosion. On the other hand, the storage capacity of the surface layer in WRC_1 is greater than in that of WRC_2, which is believed to contribute to the better performance of WRC_1. As Tami, Rahardjo, Leong, and Fredlund (2004) pointed out, the storage capacity of the relatively fine layer was one of the important parameters affecting the performance of conventional capillary barrier subject to high precipitation rates. The greater storage capacity of WRC_1 enables the cover system to sustain more severe precipitation, before the WEP is reached and preferential flow penetrating underlying layer is triggered. In addition, the fine-grained material used in the overlying layer in WRC_1 tends to have lower gas permeability in humid regions (Ng, Liu, & Chen, 2015; Vangpaisal & Bouazza, 2004). After rainfall events, the silt layer of WRC_1 tends to retain a higher volumetric water content than WRC_2 and is therefore able to better control gas release.

4.3 | Limitations

Evaporation and transpiration are of critical importance in controlling the water content and pore water pressure of soil layer (Weeks & Wilson, 2006); however, their influence was not investigated as this study focuses on the validation of cover system with water-repellent soil under rainfall. Therefore, evaporation, transpiration, and wetting–drying cycles should be taken into account when evaluating the long-term performance of cover systems with water-repellent soils. Durability of induced water repellency is another factor that affects the long-term performance of cover systems, further investigation of the long-term deterioration of coating is therefore desired. In this study, pore-water pressure data were not presented due to the early cavitation of tensiometers. It would be beneficial if pore-water pressure is measured and presented along with soil moisture data in future studies. Although this study explores the potential application of synthetic water-repellent soils in cover systems, field tests at a larger scale and extended duration are also recommended for future work. Past research has shown that numerical simulations can predict the behavior of capillary barriers and water-repellent soils with reasonable accuracy (Li, Du, Chen, & Zhang, 2013; Ritsema & Dekker, 2000). Studies are currently underway to carry out numerical simulations that assess the performance of water-repellent cover systems with various scales and initial conditions.

5 | CONCLUSIONS

A model flume was constructed, and four tests were conducted in this study to investigate the potential use of synthetic water-repellent soils in cover systems under artificial rainfall. Based on the comparison among monolithic cover, conventional capillary barrier and water-repellent cover systems, the following conclusions may be drawn:

1. Barrier effect is significantly strengthened by induced soil water repellency, including increased surface runoff, promoted lateral diversion, decreased basal percolation, and delayed breakthrough. In particular, the release of accumulated water into the underlying layer is still inhibited even after breakthrough).
2. The long-term performance of water-repellent cover system is expected to be improved, which is controlled by the underlying water-repellent layer. The deterioration resulted from desiccation cracking may be avoided.
3. A barrier can be formed using one raw material to decrease the cost for material selection and construction, by using synthetic water-repellent soil as the underlying layer.

ACKNOWLEDGMENTS

This research was supported by the Research Grants Council of Hong Kong, Grants 17205915 and T22-603/15-N. Laboratory assistance by Mr. N. C. Poon and Mr. L. H. Chan is acknowledged.

AUTHOR CONTRIBUTIONS

Shuang Zheng: Conceptualization; Data curation; Formal analysis; Investigation; Methodology; Writing-original draft. Xin Xing: Investigation; Methodology; Writing-review & editing. Sérgio D. N. Lourenço: Funding acquisition; Conceptualization; Project administration; Supervision; Writing-review & editing. Peter J. Cleall: Conceptualization; Writing-review & editing.

CONFLICT OF INTEREST

The authors declare no conflict of interest.

ORCID

Shuang Zheng https://orcid.org/0000-0001-8425-5593
Sérgio D. N. Lourenço https://orcid.org/0000-0002-7534-8760
Peter J. Cleall https://orcid.org/0000-0002-4005-5319

REFERENCES

Albright, W. H., Benson, C. H., Gee, G. W., Abichou, T., Tyler, S. W., & Rock, S. A. (2006). Field performance of three compacted clay landfill covers. *Vadose Zone Journal*, *5*, 1157–1171. https://doi.org/10.2136/vzj2005.0134

Antinoro, C., Bagarello, V., Ferro, V., Giordano, G., & Iovino, M. (2014). A simplified approach to estimate water retention for Sicilian soils by the Arya–Paris model. *Geoderma*, *213*, 226–234. https://doi.org/10.1016/j.geoderma.2013.08.004

Bachmann, J., Ellies, A., & Hartge, K. (2000). Development and application of a new sessile drop contact angle method to assess soil water repellency. *Journal of Hydrology*, *231*, 66–75. https://doi.org/10.1016/S0022-1694(00)00184-0

Bachmann, J., Woche, S. K., Goebel, M. O., Kirkham, M. B., & Horton, R. (2003). Extended methodology for determining wetting properties of porous media. *Water Resources Research*, *39*, 1353–1366. https://doi.org/10.1029/2003WR002143

Bareither, C. A., Foley, J. C., & Benson, C. H. (2016). Using surrogate meteorological data to predict the hydrology of a water balance cover. *Journal of Geotechnical and Geoenvironmental Engineering*, *142*(4). https://doi.org/10.1061/(ASCE)GT.1943-5606.0001437

Barnswell, K. D., & Dwyer, D. F. (2012). Two-year performance by evapotranspiration covers for municipal solid waste landfills in northwest Ohio. *Waste Management*, *32*, 2336–2341. https://doi.org/10.1016/j.wasman.2012.07.014

Benson, C. H., Daniel, D. E., & Boutwell, G. P. (1999). Field performance of compacted clay liners. *Journal of Geotechnical and Geoenvironmental Engineering*, *125*, 390–403. https://doi.org/10.1061/(ASCE)1090-0241(1999)125:5(390)

Benson, C. H., Sawangsuriya, A., Trzebiatowski, B., & Albright, W. H. (2007). Postconstruction changes in the hydraulic properties of water balance cover soils. *Journal of Geotechnical and Geoenvironmental Engineering*, *133* 349–359. https://doi.org/10.1061/(ASCE)1090-0241(2007)133:4(349)

Bouazza, A. (2002). Geosynthetic clay liners. *Geotextiles and Geomembranes*, *20*, 3–17. https://doi.org/10.1016/S0266-1144(01)00025-5

Chan, C. S. H., & Lourenço, S. D. N. (2016). Comparison of three silane compounds to impart water repellency in an industrial sand. *Géotechnique Letters*, *6*(4). https://doi.org/10.1680/jgele.16.00097

Czachor, H., Doerr, S., & Lichner, L. (2010). Water retention of repellent and subcritical repellent soils: New insights from model and experimental investigations. *Journal of Hydrology*, *380*, 104–111. https://doi.org/10.1016/j.jhydrol.2009.10.027

Damiano, E., Greco, R., Guida, A., Olivares, L., & Picarelli, L. (2017). Investigation on rainwater infiltration into layered shallow covers in pyroclastic soils and its effect on slope stability. *Engineering Geology*, *220*, 208–218. https://doi.org/10.1016/j.enggeo.2017.02.006

Dell'Avanzi, E., Guizelini, A., da Silva, W., & Nocko, L. (2010). Potential use of induced soil-water repellency techniques to improve the performance of landfill's alternative final cover systems. In B.O. Fityus & D. Sheng (Eds.), *Unsaturated soils* (pp. 461–466). Boca Raton, FL: CRC Press.

Doerr, S. H. (1998). On standardizing the 'water drop penetration time' and the 'molarity of an ethanol droplet' techniques to classify soil hydrophobicity: A case study using medium textured soils. *Earth Surface Processes and Landforms*, *23*, 663–668. https://doi.org/10.1002/(SICI)1096-9837(199807)23:7%3c663::AID-ESP909%3e3.0.CO;2-6

Doerr, S. H., Shakesby, R. A., Blake, W. H., Chafer, C. J., Humphreys, G. S., & Wallbrink, P. J. (2006). Effects of differing wildfire severities on soil wettability and implications for hydrological response. *Journal of Hydrology*, *319*, 295–311. https://doi.org/10.1016/j.jhydrol.2005.06.038

EPD (2019). *Restoration and afteruse of closed landfills*. Environmental Protection Department, Hong Kong Government. Retrieved from https://www.epd.gov.hk/epd/english/environmentinhk/waste/prob_solutions/msw_racl.html

Harnas, F. R., Rahardjo, H., Leong, E. C., & Wang, J. Y. (2014). Experimental study on dual capillary barrier using recycled asphalt pavement materials. *Canadian Geotechnical Journal*, *51*, 1165–1177. https://doi.org/10.1139/cgj-2013-0432

Ju, Z., Ren, T., & Horton, R. (2008). Influences of dichlorodimethylsilane treatment on soil hydrophobicity, thermal conductivity, and electrical conductivity. *Soil Science*, *173*, 425–432. https://doi.org/10.1097/SS.0b013e31817b6658

Khire, M. V., Benson, C. H., & Bosscher, P. J. (1999). Field data from a capillary barrier and model predictions with UNSAT-H. *Journal of Geotechnical and Geoenvironmental Engineering*, *125*, 518–527. https://doi.org/10.1061/(ASCE)1090-0241(1999)125:6(518)

Khire, M. V., Benson, C. H., & Bosscher, P. J. (2000). Capillary barriers: Design variables and water balance. *Journal of Geotechnical and Geoenvironmental Engineering*, *126*, 695–708. https://doi.org/10.1061/(ASCE)1090-0241(2000)126:8(695)

Laskowski, J., & Kitchener, J. A. (1969). The hydrophilic-hydrophobic transition on silica. *Journal of Colloid and Interface Science*, *29*, 670–679. https://doi.org/10.1016/0021-9797(69)90219-7

Li, J., Du, L., Chen, R., & Zhang, L. (2013). Numerical investigation of the performance of covers with capillary barrier effects in South China. *Computers and Geotechnics*, *48*, 304–315. https://doi.org/10.1016/j.compgeo.2012.08.008

Ling, H. I., Leshchinsky, D., Mohri, Y., & Kawabata, T. (1998). Estimation of Municipal Solid Waste Landfill Settlement. *Journal of Geotechnical and Geoenvironmental Engineering*, *124*, 21–28. https://doi.org/10.1061/(ASCE)1090-0241(1998)124:1(21)

McGovern, M. E., Kallury, K. M. R., & Thompson, M. (1994). Role of solvent on the silanization of glass with octadecyltrichlorosilane. *Langmuir*, *10*, 3607–3614. https://doi.org/10.1021/la00022a038

Ng, C. W. W., Liu, J., Chen, R., & Xu, J. (2015). Physical and numerical modeling of an inclined three-layer (silt/gravelly sand/clay) capillary barrier cover system under extreme rainfall. *Waste Management*, *38*, 210–221. https://doi.org/10.1016/j.wasman.2014.12.013

Ng, C. W.W., Liu, J., & Chen, R. (2015). Numerical investigation on gas emission from three landfill soil covers under dry weather conditions. *Vadose Zone Journal*, *14*(8). https://doi.org/10.2136/vzj2014.12.0180

Ng, S. H. Y., & Lourenço, S. D. N. (2016). Conditions to induce water repellency in soils with dimethyldichlorosilane. *Géotechnique*, *66*, 441–444. https://doi.org/10.1680/jgeot.15.T.025

Rahardjo, H., Prasad, A., Satyanaga, A., Mohamed, H., Leong, E.-C., Wang, C.-L., & Wong, J. L.-H. (2017). 1D infiltration behavior of two-

layered recycled concrete aggregates using hydrophobic materials in a column apparatus. *Journal of Materials in Civil Engineering*, *29*(8). https://doi.org/10.1061/(ASCE)MT.1943-5533.0001876

Rayhani, M. H. T., Yanful, E. K., & Fakher, A. (2007). Desiccation-induced cracking and its effect on the hydraulic conductivity of clayey soils from Iran. *Canadian Geotechnical Journal*, *44*, 276–283. https://doi.org/10.1139/t06-125

Ritsema, C. J., & Dekker, L. W. (2000). Preferential flow in water repellent sandy soils: Principles and modeling implications. *Journal of Hydrology*, *231–232*, 308–319. https://doi.org/10.1016/S0022-1694(00)00203-1

Ross, B. (1990). The diversion capacity of capillary barriers. *Water Resources Research*, *26*, 2625–2629. https://doi.org/10.1029/WR026i010p02625

Sadek, S., Ghanimeh, S., & El-Fadel, M. (2007). Predicted performance of clay-barrier landfill covers in arid and semi-arid environments. *Waste Management*, *27*, 572–583. https://doi.org/10.1016/j.wasman.2006.06.008

Saulick, Y., Lourenço, S. D. N., & Baudet, B. A. (2017). A semi-automated technique for repeatable and reproducible contact angle measurements in granular materials using the sessile drop method. *Soil Science Society of America Journal*, *81*, 241–249. https://doi.org/10.2136/sssaj2016.04.0131

Shaw, D. J. (1992). The solid–liquid interface. In *Introduction to colloid and surface chemistry* (4th ed., pp. 151–173). Oxford, UK: Butterworth-Heinemann.

Stormont, J. C., & Anderson, C. E. (1999). Capillary barrier effect from underlying coarser soil layer. *Journal of Geotechnical and Geoenvironmental Engineering*, *125*, 641–648. https://doi.org/10.1061/(ASCE)1090-0241(1999)125:8(641)

Stormont, J. C., & Morris, C. E. (1997). Unsaturated drainage layers for diversion of infiltrating water. *Journal of Irrigation and Drainage Engineering*, *123*, 364–366. https://doi.org/10.1061/(ASCE)0733-9437(1997)123:5(364)

Tami, D., Rahardjo, H., Leong, E. C., & Fredlund, D. G. (2004). A physical model for sloping capillary barriers. *Geotechnical Testing Journal*, *27*, 173–183.

USEPA. (2011). *Green remediation best management practices: Landfill cover systems & energy production*. Washington, DC: USEPA.

Vangpaisal, T., & Bouazza, A. (2004). Gas permeability of partially hydrated geosynthetic clay liners. *Journal of Geotechnical and Geoenvironmental Engineering*, *130*, 93–102. https://doi.org/10.1061/(ASCE)1090-0241(2004)130:1(93)

Wang, J.-P., François, B., & Lambert, P. (2020). From basic particle gradation parameters to water retention curves and tensile strength of unsaturated granular soils. *International Journal of Geomechanics*, *26*(6). https://doi.org/10.1061/(ASCE)GM.1943-5622.0001677

Wang, J.-P., Zhuang, P.-Z., Luan, J.-Y., Liu, T.-H., Tan, Y.-R., & Zhang, J. (2019). Estimation of unsaturated hydraulic conductivity of granular soils from particle size parameters. *Water*, *11*(9). https://doi.org/10.3390/w11091826

Wang, Z., Wu, L., & Wu, Q. (2000). Water-entry value as an alternative indicator of soil water-repellency and wettability. *Journal of Hydrology*, *231*, 76–83. https://doi.org/10.1016/S0022-1694(00)00185-2

Weeks, B., & Wilson, G. W. (2006). Prediction of evaporation from soil slopes. *Canadian Geotechnical Journal*, *43*, 815–829. https://doi.org/10.1139/t06-049

Wijewardana, N. S., Müller, K., Moldrup, P., Clothier, B., Komatsu, T., Hiradate, S., … Kawamoto, K. (2016). Soil-water repellency characteristic curves for soil profiles with organic carbon gradients. *Geoderma*, *264*, 150–159. https://doi.org/10.1016/j.geoderma.2015.10.020

Zheng, S., Lourenço, S. D. N., Cleall, P. J., Chui, T. F. M., Ng, A. K. Y., & Millis, S. W. (2017). Hydrologic behavior of model slopes with synthetic water repellent soils. *Journal of Hydrology*, *554*, 582–599. https://doi.org/10.1016/j.jhydrol.2017.09.013

Zornberg, J. G., LaFountain, L., & Caldwell, J. A. (2003). Analysis and design of evapotranspirative cover for hazardous waste landfill. *Journal of Geotechnical and Geoenvironmental Engineering*, *129*, 427–438. https://doi.org/10.1061/(ASCE)1090-0241(2003)129:6(427)

How to cite this article: Zheng S, Xing X, Lourenço SDN, Cleall PJ. Cover systems with synthetic water-repellent soils. *Vadose Zone J*. 2020;e20093. https://doi.org/10.1002/vzj2.20093